Appl Phys A
DOI 10.1007/s00339-008-4992-2

Applied Physics A
Materials Science & Processing

Influence of self-assembled monolayer chain length on modified gate dielectric pentacene thin-film transistors

I.G. Hill · C.M. Weinert · L. Kreplak · B.P. van Zyl

Received: 14 July 2008 / Accepted: 24 November 2008
© Springer-Verlag 2008

Abstract Self-assembled monolayers are widely used to modify the gate dielectric/semiconductor interface in organic thin-film transistors. By modifying the interaction between the molecular semiconductor and the substrate, thin-film ordering and the electronic properties of the semiconducting channel can be controlled. The modified semiconductor/dielectric properties result in macroscopically observed changes in the charge-carrier mobilities, threshold voltages, subthreshold swing and transfer characteristic hysteresis. The latter two are determined by the density of charge-trapping states at the interface. Here, we investigate the influence of the thickness of the self-assembled monolayer, via the alkyl chain length in n-alkyl phosphonic acid-based monolayers on SiO_2, on the electronic properties of pentacene-based organic thin-film transistors. Rather than a monotonic increase or decrease in performance with increasing chain length, we have found that the optimum performance occurs with chains of 8–10 carbon atoms. Atomic force microscopy shows a correlation between pentacene crystalline grain size and transistor performance.

PACS 85.30.Tv · 85.30.-z · 81.15.Cd · 68.55.Nq · 42.70.Jk

Organic thin-film transistors (OTFTs) are an alternative technology to amorphous silicon thin-film transistors (a-Si TFTs) in large-area electronic devices, such as active-matrix displays. OTFT fabrication processes are free of high-temperature processing steps, unlike their inorganic counterparts. This allows the use of low-cost flexible substrates such as polyethylene terephthalate (PET) and naphthalate [1], enabling large-scale, low-cost roll-to-roll continuous manufacturing processes, potentially resulting in a greatly reduced cost per unit area for the completed circuits.

OTFTs based on polycrystalline thin films of pentacene and its derivatives exhibit performance metrics which are virtually identical to those of their a-Si counterparts [1–4]. These p-channel devices have carrier mobilities in the range of 1 $cm^2/V\,s$ and on–off ratios between 10^6 and 10^8. Unfortunately, the subthreshold performance of pentacene OTFTs is typically inferior to a-Si TFTs. Subthreshold swings can be several volts per decade, and positive threshold voltages on the order of tens of volts are typical of OTFTs constructed on 350-nm-thick SiO_2 dielectrics [2]. Both the poor subthreshold swings and the large threshold voltage shifts are caused by a high density of charge-trapping states either in the channel or at the semiconductor/gate dielectric interface [5, 6]. The origin of these charge-trapping states may be related to poor crystalline ordering and grain boundary derived gap states, or they may be due to interface gap states caused by the interaction between the semiconducting molecules and the polar SiO_2 surface.

Self-assembled monolayers (SAMs) based on trichlorosilane [2], phosphonic acid [4, 7–10] and trimethoxysilane [11] binding groups (to name a few) have been very successful at improving the subthreshold performance. Here, the hydrophilic SiO_2 surface is replaced with a hydrophobic SAM, improving the wetting by the organic semiconductor molecules and presumably resulting in improved order in the first few monolayers that form the channel. Even with relatively thick (100-nm) SiO_2 dielectrics, devices with

I.G. Hill (✉) · C.M. Weinert · L. Kreplak
Department of Physics, Dalhousie University, Halifax, Canada
e-mail: ian.hill@dal.ca

B.P. van Zyl
Department of Physics, St. Francis Xavier University, Antigonish, Canada

Published online: 16 December 2008

subthreshold swings only a few times the thermodynamically allowed minimum of 58 meV/decade [4] and uniform, slightly negative threshold voltages have been reported. It has also been suggested that a large density of electron-trapping states at organic/SiO_2 interfaces are due to surface hydroxyl groups [12]. Systematic studies of both SAM-treated SiO_2 dielectrics and polymer dielectrics with and without hydroxyl groups indicated a clear correlation between the subthreshold metrics and the presence or absence of n-channel conductance due to strong electron trapping. Electron traps with long detrapping times (compared to the length of an experiment) in a p-channel device will result in threshold voltage hysteresis between on-to-off and off-to-on sweeps, in that order. The electron traps are not populated until a positive (off) gate bias is applied. Therefore, the on-to-off sweep is not affected by the trapped charge density, while the off-to-on sweep is. The presence of this net charge density on one side of the gate/dielectric/channel capacitor results in a built-in potential that shifts the threshold voltage, resulting in hysteresis between the sweeps. The density of charge-trapping states can be estimated from both the subthreshold swing and the threshold voltage shift [5].

The majority of SAMs studied in the literature have consisted of the binding group and an octadecyl chain, such as octadecyl trichlorosilane, octadecyl phosphonic acid and octadecyl trimethoxysilane [2, 8–11]. The influence of the alkyl chain length on the electronic properties of the semiconductor overlayer has not been reported. In this work we report the properties of pentacene OTFTs constructed using n-alkyl phosphonic acid SAM-modified SiO_2 gate dielectrics with alkyl chains containing even numbers of carbon atoms from 6 to 18, effectively controlling the thickness of the organic buffer layer between the polar SiO_2 surface and the organic semiconducting channel. Intuitively, one expects the screening of the SiO_2 surface to improve with increasing buffer layer thickness, and a concomitant improvement of the electronic properties of the semiconducting overlayer.

Pentacene OTFTs were fabricated on heavily doped Si wafers (p-type; boron; $<0.005\ \Omega\,\mathrm{cm}$) with 100-nm thermal oxide. The Si wafer served as a common gate electrode for all transistors, and the thermal oxide as the gate dielectric. Si coupons were sonicated in methanol and immediately blown dry with dry compressed air followed by oxygen plasma cleaning in a parallel-plate reactive-ion etcher (Trion Technologies Phantom) at 250 W rf power, 200 mTorr and 20 sccm O_2 for 1 min. After removal from the etcher, the coupons were immediately immersed in 0.5 mmol solutions of the n-alkyl phosphonic acids (Strem Chemical) in 2-propanol for 43 h. Following SAM deposition, the coupons were annealed under rough vacuum for 10 min at 145°C, rinsed in clean 2-propanol and immediately blown dry. In addition to the SAM coupons, control coupons underwent the same procedure, immersed in neat 2-propanol instead of an n-alkyl phosphonic acid solution. SAM-coated coupons were characterized by deionized water contact angle measurements (Fig. 1). The error bars represent the range of values measured for three different locations on the coupon. There is a slight trend towards larger contact angles with increasing chain length, from ≈96° for hexyl phosphonic acid to ≈102° for octadecyl phosphonic acid, indicating decreasing electrostatic interaction with the polar SiO_2 surface beneath with increasing buffer layer thickness. Note that even the control sample, immersed only in 2-propanol, still exhibits a relatively large contact angle of 63°, compared to the vanishingly small angles expected for oxygen plasma cleaned SiO_2, indicating that some species remain on the surface following immersion in the 2-propanol. The contact angle of the control is much smaller than those of the SAMs, however, clearly demonstrating the effect of the SAMs.

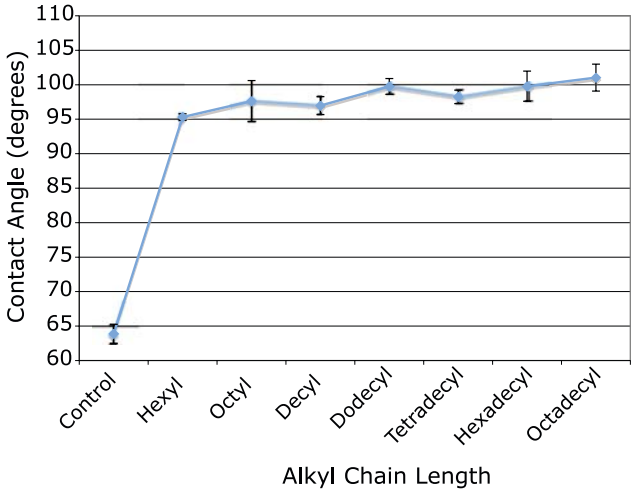

Fig. 1 Water contact angles for each of the n-alkyl phosphonic acid SAMs and the control (Nanopure; 18.2 MΩ). *Data points* represent the average of three measurements and the *error bars* the range

Pentacene (sublimed grade; America Organic Semiconductor) was deposited by thermal vacuum deposition (base pressure 7×10^{-7} Torr; $<5 \times 10^{-6}$ Torr during deposition) at a rate of 0.1 nm/s to a total thickness of 50 nm with the substrate held at 70°C. The pentacene was patterned through a stencil mask to minimize leakage currents. Two coupons were included in each run. To avoid any systematic errors from run to run that may be confused with chain length dependent properties, the following pairings were used: hexyl and octadecyl, octyl and hexadecyl, decyl and tetradecyl, dodecyl and control. Following pentacene deposition and cooling of the substrates to below 40°C, vacuum was broken and the pentacene mask was replaced with a source–drain stencil mask. Gold source–drain electrodes, 50-nm thick, were deposited at 0.1 nm/s at a vacuum better than 5×10^{-6} Torr with the sample holder nominally at room temperature. An array of top-contact transistors with

channel lengths of 100 μm and 250 μm, and channel widths of 1.5 mm, 1 mm and 0.5 mm, was fabricated on each coupon.

Electronic characteristics of the pentacene OTFTs were measured using two Keithley 236 source-measure units (SMUs)— one to control the source–drain voltage and measure the drain current, and one to control the source–gate voltage and measure the gate leakage current. The saturation transfer curves were measured by applying −25 V to the drain and sweeping the gate from −25 V to +25 V and back for the on-to-off and off-to-on scans, respectively. The sweep rate is dependent on the integration time of the Keithley 236 SMUs, which is dynamically adjusted, depending on the magnitude of the current being measured. For most of the sweep, an effective rate of 2 V/s was used, although it was as low as 0.5 V/s in the 'off' region, where the currents are very small. Device parameters were not studied as functions of sweep rate. The threshold voltages and hole mobilities were extracted from the saturation transfer curves from the intercept and slope, respectively, of the linear portion of the square root of the drain current as a function of gate voltage, assuming the ideal p-channel FET equations to hold:

$$i_{\mathrm{DS}}^{\mathrm{sat}} = \frac{1}{2}\mu C_{\mathrm{ox}}\frac{W}{L}(V_{\mathrm{GS}} - V_{\mathrm{T}})^2, \quad V_{\mathrm{DS}} < V_{\mathrm{GS}} - V_{\mathrm{T}}. \tag{1}$$

A typical saturation transfer curve, plotted both on a logarithmic scale and as the square root of the drain current, is included in Fig. 2 to illustrate and justify the validity of the method. The data was collected from an octyl phosphonic acid modified transistor with $W/L = 6$. A small degree of hysteresis is evident, which results in a threshold voltage shift of approximately +1.8 V between the on-to-off and off-to-on transfer curves, collected in that order. The mobility and subthreshold swing data, as functions of the alkyl chain length, are plotted in Fig. 3. The data points represent the average values for each sample and the error bars are drawn to indicate the total range of values measured. For consistency, the values plotted for each sample are derived from the off-to-on transfer curves. Referring to Fig. 3a, note that the mobilities measured for all eight samples are $\gtrsim$0.3 cm^2/V s, and therefore well within the accepted literature range for polycrystalline pentacene thin films. A definite maximum is evident, however at a chain length of C-8, octyl phosphonic acid. Here, all transistors demonstrated mobilities in excess of 1 cm^2/V s, and the best devices nearly 2 cm^2/V s. For alkyl chains longer than C-8, the average mobilities monotonically decrease, again reaching 0.3 cm^2/V s for C-18. The subthreshold swings, on the other hand, are ≈0.9 V/decade for the 2-propanol control, 0.6 V/decade for C-6, and all longer alkyl chain SAM substrates are consistent with an average of 0.5 V/decade, with some devices as low as 0.4 V/decade, indicating a substantially lower trap density resulting from the introduction of the SAMs. It is

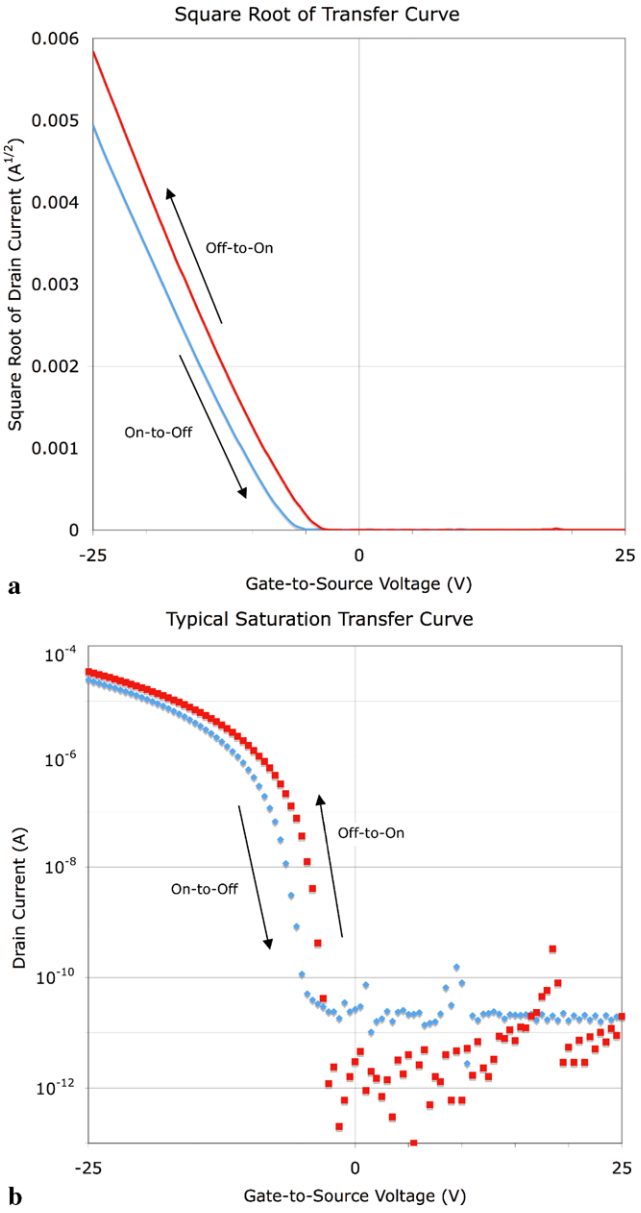

Fig. 2 On-to-off and off-to-on saturation transfer curves of a typical n-alkyl SAM modified pentacene OTFT. This data was collected from an octyl phosphonic acid transistor with a W/L of 6. **a** Square root of the drain current as a function of gate–source voltage. **b** Drain current plotted on a logarithmic scale. The drain is held at −25 V with respect to the source

interesting to note, however, that while the control device and the C-14, C-16 and C-18 SAM devices all have approximately the same mobilities, the trap density appears to be much lower for the SAM devices than for the control, indicating that the mobility in the latter devices does not appear to be limited by the density of charge-trapping states.

The threshold voltage shifts, defined as the difference between the measured off-to-on and on-to-off threshold voltages, are included in Fig. 4, along with the maximum on/off ratio measured for each sample. Qualitatively, we see a sim-

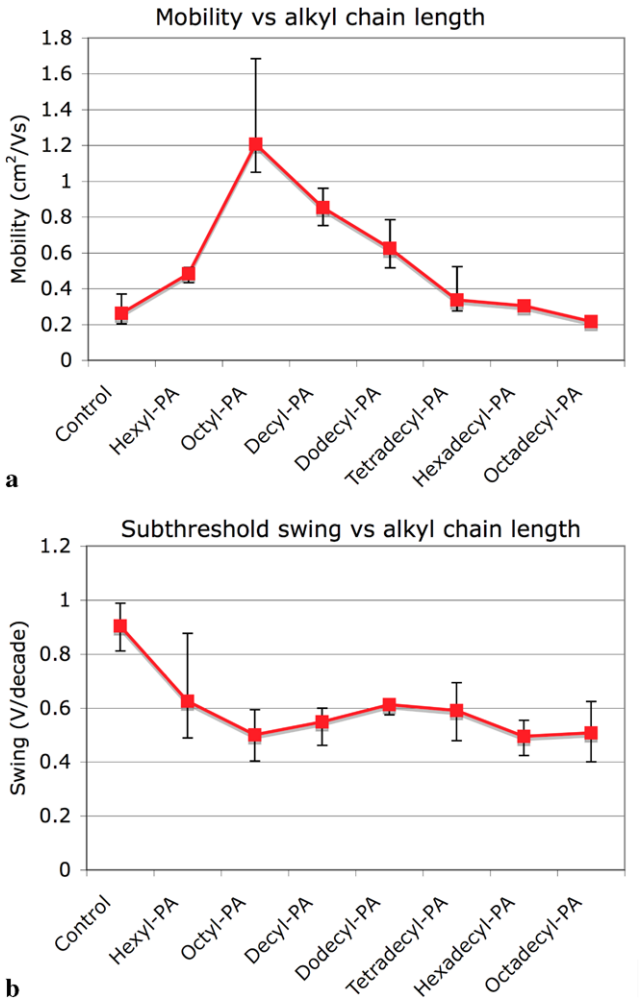

Fig. 3 Variation of hole mobility and subthreshold swing with alkyl chain length for off-to-on transfer characteristics. *Data points* are average values and *error bars* indicate the observed range

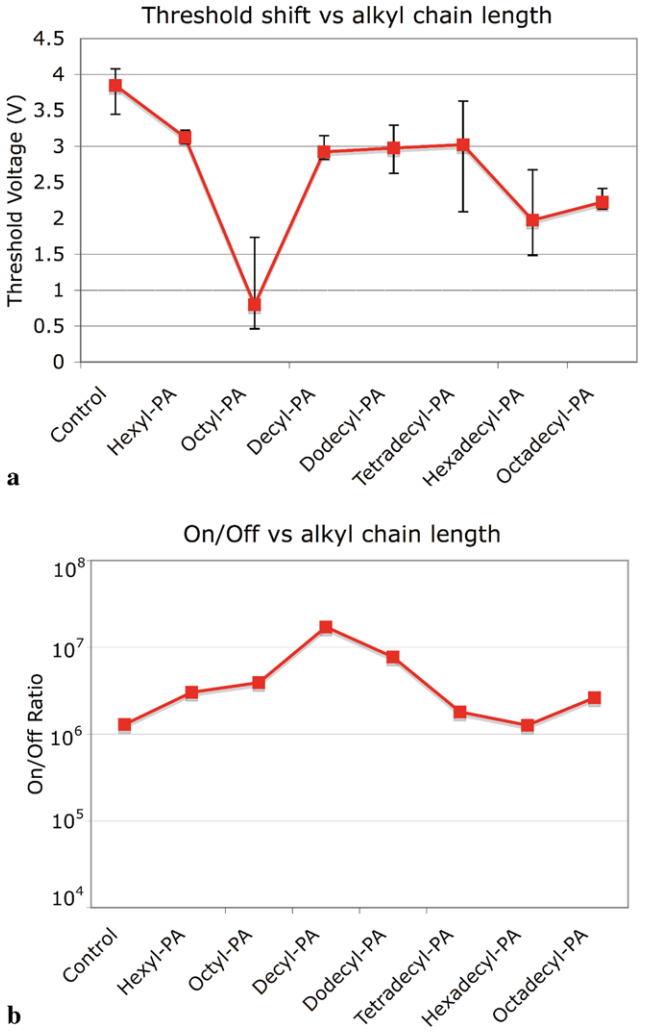

Fig. 4 Variation of threshold voltage shift and on/off ratio with alkyl chain length. The threshold voltage shift is defined as the threshold voltage for the off-to-on sweep minus that for the on-to-off sweep. The difference between the two indicates the degree of hysteresis. Threshold shifts represent the average (*points*) and range (*error bars*) observed, while the on/off ratios are the best values observed

ilar indication of the variation of trap density with alkyl chain length. The degree of hysteresis is greatest for the 2-propanol control (≈4 V), least for the octyl phosphonic acid (≈1 V, although with a sizable range) and consistent with a mean value of ≈2.5 V for all other chain lengths.

To gain further insight into the differences between the pentacene films grown on the treated substrates, contact mode atomic force microscopy (AFM; Agilent 5500 with Nanoworld PointProbes cantilevers ≈0.2 N/m) was performed on the channel regions of individual devices. It must be remembered that the degree of ordering observed by AFM at the top of the 50-nm-thick pentacene film does not necessarily reflect the ordering in the first few nanometers that form the transistor channel and determine the electronic properties of the device. 5 μm × 5 μm topology images from the control, hexyl, decyl, tetradecyl and octadecyl phosphonic acid-modified devices are included in Fig. 5. Figure 5 also includes a deflection image (panel B) for the 2-propanol control, which highlights the clearly visible steps and terraces that are present in all images. The steps are ≈1.5 ± 0.2 nm in height, consistent with the tilted monomolecular length, or half of the pentacene triclinic cell *c*-axis lattice parameter. By examining the apparent grain size as a function of alkyl chain length, we see a clear trend. Intermediate chain lengths produce large, well-ordered dendritic grains several microns in size, while the longer chains result in submicron-sized grains ≈200–300 nm in size with a more granular appearance. The 2-propanol control produced intermediate results, with grain sizes ≈600–800 nm. Upon closer scrutiny, however, one may note that although the grains are much larger and better defined for the hexyl phosphonic acid treated sample compared to either the 2-propanol control or the tetradecyl phosphonic acid sample, the mobilities are not that different. The grains are almost identical for the hexyl

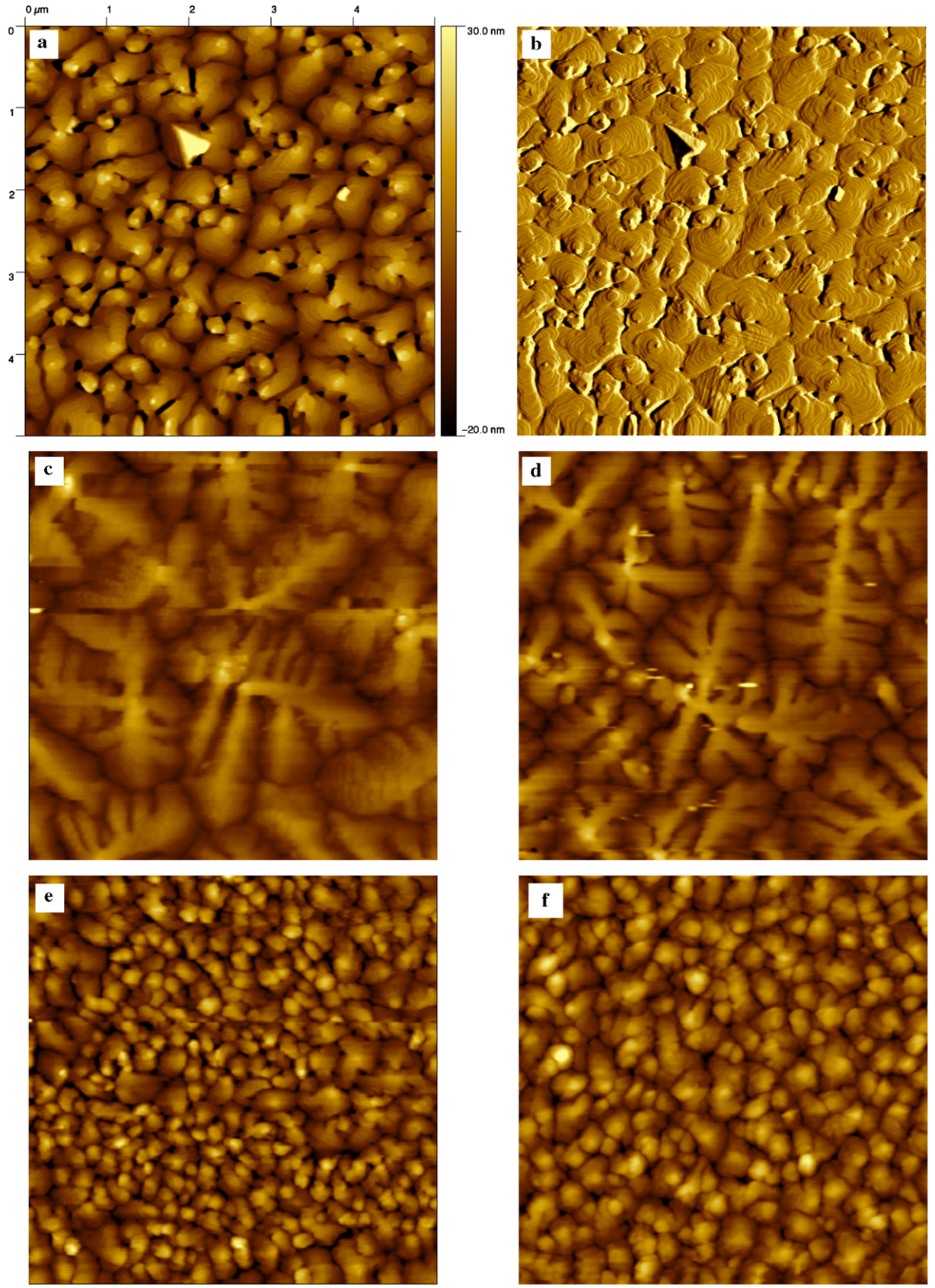

Fig. 5 AFM images of pentacene film on (**a**) 2-propanol control, (**b**) 2-propanol: deflection image showing steps and terraces, (**c**) hexyl phosphonic acid, (**d**) decyl phosphonic acid, (**e**) tetradecyl phosphonic acid and (**f**) octadecyl phosphonic acid

and decyl phosphonic acid substrates, but the mobility of the decyl phosphonic acid devices is much larger. Furthermore, although the tetradecyl and octadecyl phosphonic acid samples have significantly smaller grain sizes compared to the 2-propanol control, they have comparable mobilities, and the SAM-treated samples have uniformly better subthreshold swings and lower threshold voltage hysteresis than the untreated sample. Note that we cannot eliminate the possible interpretation of voids between the pentacene grains resulting in poor intergrain transport. The morphology of the first mono/multilayers of pentacene at the dielectric interface cannot be accurately probed by AFM images of the 50-nm-thick films. From these images and the electronic properties of the corresponding transistors, we see that there is no clear correlation between grain size and average hole mobility in these devices, in contrast to some earlier reports [13] but in agreement with others [14]. Our interpretation of these results will be discussed in the following paragraph. Obviously, care must be taken when predicting the electronic properties of the film based solely on the AFM-determined grain structure.

We propose that there are two dominant mechanisms that limit the performance of the devices with lower mobility, result in trapping states that degrade the subthreshold performance and cause threshold voltage hysteresis. We consider shallow, short-lived hole traps that degrade both the macroscopic mobility and the subthreshold performance, but do not impact the hysteresis, as their mean trapping times are small compared to the length of time required to perform a transfer curve measurement. Deep, long-lived electron traps, on the other hand, will produce the threshold voltage shifts and hysteresis between the on-to-off and off-to-on sweeps observed [6]. The presence of charged deep electron traps has also been found to reduce the average hole mobility, due to the creation of shallow hole trap states caused by the electrostatic interaction of the hole with the negatively charged occupied electron trap [15]. Considering these two types of traps, we can qualitatively understand the behavior of our devices. The 2-propanol control devices appear to have a larger density of deep electron traps, perhaps arising from the interaction of the pentacene molecules with the polar SiO_2 surface. As indicated by the contact angle measurements, even though the 2-propanol-treated surface is not pristine SiO_2, it is still much more hydrophilic than any of the SAM-treated surfaces. These trapping states result in the (relatively) poor subthreshold performance, the threshold voltage hysteresis and the reduced mobility. On the other hand, the longer chain alkyl phosphonic acid devices have relatively good subthreshold performance and less hysteresis, but reduced mobility originating from a high density of shallow hole trap states, perhaps due to the high density of pentacene grain boundaries present. We hypothesize that the longer chain phosphonic acid molecules result in poorer ordering in the SAM compared to the intermediate chains. These SAM defect sites then act as nucleation sites for pentacene grains. The high density of nucleation sites results in smaller grains on average. The optimum performance observed at intermediate chain lengths is then the best compromise, with a sufficiently hydrophobic surface and better ordering than the longer chain SAMs. It should be noted, however, that this suggestion of poorer ordering with increasing chain length between the hexyl and octadecyl chain lengths contradicts the well-accepted result that SAM ordering improves in this range for alkane thiols on single-crystal gold. In fact, Camillone et al. found that the ordering of alkane thiol monolayers on Au(111) degrades for chains with less than 10 C atoms/chain due to decreasing interchain interaction [16]. It is not unreasonable, however, to suggest that growth on an amorphous substrate such as SiO_2 with a different binding group may alter the ordering of the SAM and account for the difference between the gold/thiol results and those presented here. Alternatively, the less well ordered SAMs produced at shorter chain lengths may actually be more conducive to the growth of a large-grained pentacene overlayer. In order to test these hypotheses, further experiments to investigate the early stages of pentacene film growth on these SAMs and electrical measurements to determine the energy distribution and density of trapping states are required.

Acknowledgements This work was supported by the Natural Sciences and Engineering Research Council of Canada and the Canada Foundation for Innovation. The authors wish to thank Prof. H. Rotermund for the use of his AFM facility.

References

1. C.D. Sheraw, L. Zhou, J.R. Huang, D.J. Gundlach, T.N. Jackson, M.G. Kane, I.G. Hill, M.S. Hammond, J. Campi, B.K. Greening, J. Francl, J. West, Appl. Phys. Lett. **80**, 1088 (2002)
2. Y.-Y. Lin, D.J. Gundlach, S.F. Nelson, T.N. Jackson, IEEE Electron Device Lett. **18**, 606 (1997)
3. M. Shtein, J. Mapel, J.B. Benziger, S.R. Forrest, Appl. Phys. Lett. **81**, 268 (2002)
4. M. McDowell, I.G. Hill, J.E. McDermott, S.L. Bernasek, J. Schwartz, Appl. Phys. Lett. **88**, 073505 (2006)
5. A. Bolognesi, M. Berliocchi, M. Manenti, A.D. Carlo, P. Lugli, K. Lmimouni, C. Dufour, IEEE Trans. Electron Devices **51**, 1997 (2004)
6. G. Gu, M.G. Kane, J.E. Doty, A.H. Firester, Appl. Phys. Lett. **87**, 243512 (2005)
7. I.G. Hill, J. Hwang, A. Kahn, C. Huang, J.E. McDermott, J. Schwartz, Appl. Phys. Lett. **90**, 012109 (2007)
8. J.E. McDermott, M. McDowell, I.G. Hill, A. Kahn, S.L. Bernasek, J. Schwartz, J. Phys. Chem. A **111**, 12333 (2007)
9. H. Klauk, U. Zschieschang, M. Halik, J. Appl. Phys. **102**, 074514 (2007)
10. H. Klauk, U. Zschieschang, J. Plaum, M. Halik, Nature **445**, 745 (2007)

11. A. Matsumoto, R. Onoki, S. Ikeda, K. Saiki, K. Ueno, Jpn. J. Appl. Phys. Part 2—Lett. Express Lett. **46**, L913 (2007)
12. L.-L. Chua, J. Zaumseil, J.-F. Chang, E.C.-W. Ou, P.K.-H. Ho, H. Sirringhaus, R.H. Friend, Nature **434**, 194 (2005)
13. R. Matsubara, N. Ohashi, M. Sakai, K. Kudo, M. Nakamura, Appl. Phys. Lett. **92**, 242108 (2008)
14. M. Shtein, J. Mapel, J.G. Benziger, S.R. Forrest, Appl. Phys. Lett. **81**, 268 (2002)
15. S.O. Kasap, C. Juhasz, J. Phys. D: Appl. Phys. **18**, 703 (1985)
16. N. Camillone, C.E.D. Chidsey, G.Y. Liu, T.M. Putvinski, G. Scoles, J. Chem. Phys. **94**, 8493 (1991)